Charge transfer and electron detachment for collisions of H^- and D^- with H

M. A. Huels, R. L. Champion, L. D. Doverspike, and Yicheng Wang
Department of Physics, College of William and Mary, Williamsburg, Virginia 23185
(Received 17 November 1989)

Total cross sections for charge transfer and electron detachment for collisions of H^- and D^- with atomic hydrogen have been separately determined for collision energies that range from a few electron volts up to several hundred electron volts. The experiments are performed with an apparatus that utilizes a crossed-beam configuration with a radio-frequency discharge as the source of atomic hydrogen. The experimental results are compared with several calculations and with other measurements that overlap the present results at the highest collision energies.

I. INTRODUCTION

The system of H^-+H is the most fundamental negative ion-atom combination, yet despite the conceptual simplicity of this system, it presents some of the most vexing difficulties, both from an experimental and theoretical point of view. Due to the inherent difficulty of producing intense, well-characterized beams of hydrogen atoms at room temperature, investigations of low-energy collisions of negative ions with atomic hydrogen have been few and mostly emphasized energies above 500 eV. Recent developments in the area of merged beams[1] may remedy this deficiency.

In a low-energy collision of H^- with H there are several processes which are of fundamental interest: associative detachment,

$$H^-+H\rightarrow H_2+e^- , \tag{1}$$

direct detachment,

$$H^-+H\rightarrow H+H+e^- , \tag{2}$$

and charge transfer,

$$H^-+H\rightarrow H+H^- . \tag{3}$$

These three reactions are of great importance in the physics of stellar atmospheres and, in particular, in the calculation of stellar absorption coefficients and opacities. It is well known that these reactions and the reverse of (1), i.e., dissociative attachment, play vital roles in determining the equilibrium densities of H^- and electrons in the solar chromosphere.[2-4]

Reaction (1) has been studied theoretically by Bieniek and Dalgarno[5] and Browne and Dalgarno,[6] and its thermal rate constant has been determined by Schmeltekopf *et al.*[7] In fact the H_2^- system has received attention primarily in the context of e^-+H_2 collisions, both theoretically[8,9] and experimentally,[10] and although the calculations reproduce qualitative aspects of this scattering process, they do not predict the correct isotope shift. The processes of direct detachment and charge transfer for H^-+H have also received considerable attention. Based on a general theory first elaborated by Massey and Smith,[11] Mott and Massey,[12] and Bates, Massey and Stewart,[13] charge transfer cross sections have been reported by Dalgarno and McDowell[14] for collision energies between 10 eV and 10 keV. Experimentally, Hummer *et al.*[15] have found good agreement with those calculated cross sections for charge transfer for energies between 0.1 to 1.0 keV, and fair agreement for the energy range from 1.0 to 10 keV. Their results show that the charge-transfer cross section $\sigma_{CT}(E)$ decreases monotonically with increasing energy up to 1.0 keV, whereas above that energy $\sigma_{CT}(E)$ falls off faster than predicted, mainly due to the failure of the perturbed stationary state (PSS) theory to allow for momentum transfer. Hummer *et al.* also reported direct detachment cross sections $\sigma_e(E)$ over the same energy range and they are in good agreement with the calculated cross sections of Bardsley[16] in the energy range between 0.4 and 2.0 keV. These latter calculations, based upon a local complex potential (LCP) model, are for energies up to 10 keV and predict that $\sigma_e(E)$ should also decrease monotonically with increasing energy. Above 2.0 keV however, the direct detachment cross sections measured by Hummer *et al.* appear to agree qualitatively more with calculations using the Born approximation by McDowell and Peach.[17] Bardsley also reevaluated the charge-transfer cross sections of Dalgarno and McDowell by incorporating his results for electron detachment and found excellent agreement with the experimental results of Hummer *et al.*,[15] in particular at energies above 1.0 keV.

Other descriptions of electron detachment within the framework of the LCP model have been made by Browne and Dalgarno[6] who studied the relative contributions of the $^2\Sigma_u$ and $^2\Sigma_g$ states of H_2^- to the electron-detachment cross section. Their calculated detachment cross section showed the usual decrease with increasing energy above about 100 eV, but a relatively constant cross section of about 15 $Å^2$ between approximately 100 and 10 eV and decreasing below 10 eV.

The difficulty in theoretically assessing the charge-transfer and electron-detachment cross sections for H^-+H lies mainly in the problems associated with determining the energies of the H_2^- resonant states. Figure 1 shows a schematic of the two lowest states of H_2^- and

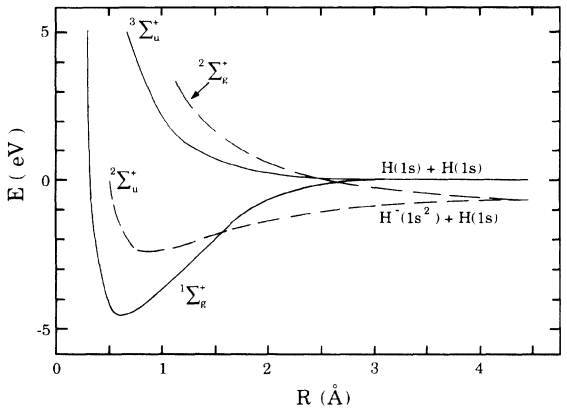

FIG. 1. Schematic of the two lowest states of H_2 (Ref. 18) and H_2^- (Refs. 9 and 29).

H_2.[18] Substantial disagreements exist between the calculated states of H_2^- (see Amaya-Tapia *et al.*[19] and references cited therein for an excellent discussion on this point), in general in regard to the crossings of the $^2\Sigma_u$ and $^2\Sigma_g$ states of H_2^- with the H_2 continuum and, in particular, the magnitude of the energy of the $^2\Sigma_u$ state.[20] It is clear, however, that the molecular anion becomes unstable where the $^2\Sigma_{g,u}$ states of H_2^- cross into the continuum representative of H_2+e.

At present, not many experiments have been reported which further elaborate on the results of Hummer *et al.*[15] Geddes *et al.*[21] studied total stripping and H^+ production in collisions of H^-+H in the 1–300-keV range, and Gealy *et al.*[22] determined total neutralization cross sections for H^-+H over the energy range from approximately 60 eV to 2 keV. Although the latter measurements extend far lower in energy than those of Hummer *et al.*, the individual contributions of charge transfer and electron detachment to the total neutralization were not determined. Esaulov[23] has reported differential electron-detachment cross sections of H^-+D and D^-+H, and his work suggests that σ_e does not increase with decreasing energy but remains relatively constant down to about 100 eV. Indeed Esaulov concludes that his results are "contrary to the prediction of the LCP model and it seems desirable that a thorough measurement of this cross section (σ_e) at low energies be performed."

In this paper, we report measurements of the total electron-detachment and charge-transfer cross sections for collisions of H^- and D^-+H, for laboratory energies from 7 eV up to 400 eV.

II. EXPERIMENTAL APPARATUS AND PROCEDURE

As shown in Fig. 2, the device used for the total cross-section measurements is of the crossed-beam configuration. The negative ions H^- and D^- are produced in an arc-discharge source (a) of a type which has been used previously in this laboratory in a number of studies involving collisions of negative ions with gaseous targets.[24–26] The source gas consists of a mixture of Ar, H_2, and D_2 in the ratios 2:1:1. After extraction the H^- or D^- ions are mass selected (b) and subsequently focused by a series of Einzel lenses (c).

The ion beam is focused through a 1.3-mm aperture and enters the scattering region which consists of a 30° section of a cylindrical electrostatic energy analyzer with a radius of curvature of 76 mm. The voltage across the two curved plates, V_n and V_p, are chosen such that the ion beam will pass resonantly through the analyzer. The transmitted primary ion beam is monitored by a Faraday cup (f), and the laboratory energy distribution may be determined by a series of grids, (g_1) and (g_2), before and after the primary ion beam passes through the collision region.

The maximum beam intensities of H^- and D^- for this particular ion source are about 0.5 nA, and the energy spread of the ion beam ranges between 1 eV for the lowest collision energy and 5 eV for the highest.

The grids (g_1) just before the Faraday cup also serve to suppress any secondary electrons produced by collisions of the ion beam with the Faraday cup.

Halfway through the cylindrical-analyzer section the ion beam and neutral target beams intersect orthogonally. The transverse field maintained across the curved plates (n) and (p) allows the slow product ions and electrons to be extracted perpendicularly to the plane defined by the reactants. The collision products, after focusing by an Einzel lens (d) pass through a region of magnetic field (e) which separates electrons from those product ions which are a result of charge transfer. The scattered products are detected by conventional particle multipliers (h) and their outputs are amplified in vacuum (i) to reduce rf-related noise.

The atomic hydrogen beam is produced in a commercially available source (j), briefly described below. The source may be positioned under vacuum conditions, allowing a separate gas nozzle (k) to be moved into place, thus making it possible to introduce an alternate target gas into the scattering region. The relative collection efficiencies for the product anion and electron detection systems, at a given collision energy, are determined by normalization to the known total cross sections $\sigma_e(E)$ and $\sigma_{CT}(E)$ for H^-+O_2.[25] These two cross sections are comparable in magnitude over the energy range of interest. The normalization procedure yields energy-dependent transmission functions for the product anion and electron detection systems. The transmission function for anions is slightly different from that for electrons; however, the ratio of these transmission functions is found to deviate from unity by no more than 12% over the energy range of $5 < E < 300$ eV.

The neutral hydrogen atom beam source is of the rf discharge type and has been described in detail elsewhere.[27] High purity H_2 is admitted by a paladium leak into the discharge region which is surrounded by a water-cooled jacket and rf resonator. The discharge is struck by feeding 20–30 W of rf power into the resonator at a frequency of about 36 MHz. Once the discharge stabilizes, the input power can be reduced to about 11 W and the rf frequency may be tuned to achieve maximum absorption of the rf power. The dissociation fraction is

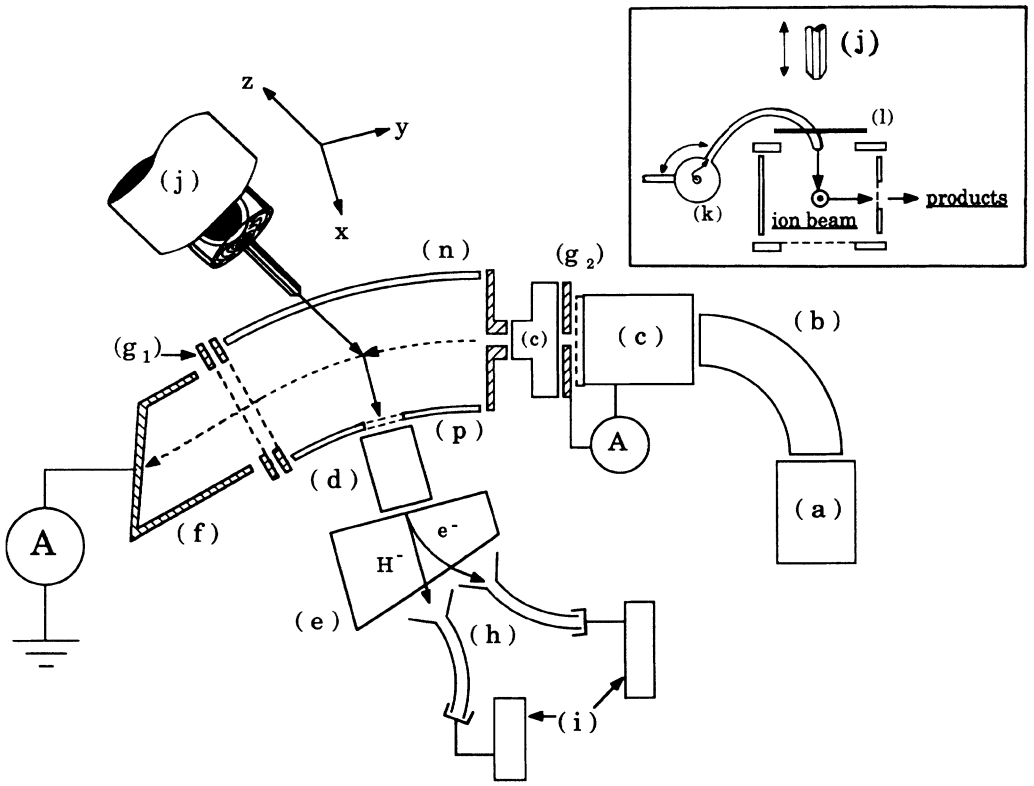

FIG. 2. Schematic diagram of the crossed-beam apparatus: (*a*) arc discharge source, (*b*) momentum analyzer, (*c*) and (*d*) Einzel lenses, (*e*) separator magnet, (*f*) Faraday cup, (g_1) and (g_2) grids, (*h*) particle detectors, (*i*) amplifiers, (*j*) rf discharge atomic hydrogen source, (*n*) and (*p*) deflector-extraction plates, (*k*) rotatable gas nozzle, and (*l*) top electrostatic shield.

found to be as high as 88% and its determination shall be discussed at a later point. The hydrogen atoms and residual H_2 molecules effuse from the discharge region through a 2-mm bore capillary, which contains a bend "to reduce uv light leakage from the discharge,"[28] followed by an exit capillary of about 20-mm length and 1-mm bore. The lower part of the rf source is clad in a copper shield which serves as additional rf shielding and also prevents charge buildup on the exit nozzle. In the present configuration the atomic hydrogen source is joined to the vacuum system by means of a precision three-dimensional manipulator.

To insure that the inside of the rf discharge source is free of contaminants, which is essential for low recombination rates on the surface, three procedures are of utmost importance: (i) a positive pressure must always be maintained inside the pyrex source tube, typically about 0.1 torr, with respect to the background pressure inside the target chamber of approximately 6×10^{-7} torr; (ii) the entire vacuum system is roughed down from atmosphere through a liquid nitrogen trap; and (iii) venting occurs only with dry nitrogen.

To determine the dissociation fraction f of the target beam, i.e., the percentage of H_2 molecules dissociated, recent measurements by Gealy *et al.*[22] for the total neutralization cross sections for $H^-+H(\sigma_H)$ and $H^-+H_2(\sigma_{H_2})$ are used. The collisional products collected with the rf power off are

$$I_{\text{off}}=kn\sigma_{H_2}\,, \tag{4}$$

where n is the number density of H_2 and the proportionality constant k depends on the primary ion beam intensity, geometrical target thickness, and the product collection efficiency of the apparatus. With rf on, the density of H_2 is reduced to $(1-f)n$ and the resultant density of H is $(2/2^{1/2})nf$, assuming that the thermal kinetic energy of the target particles remains the same. The collisional products are then

$$I_{\text{on}}=kn[(1-f)\sigma_{H_2}+2^{1/2}f\sigma_H]\,. \tag{5}$$

Relations (4) and (5) yield the dissociation fraction

$$f=(I_{\text{on}}/I_{\text{off}}-1)/[2^{1/2}(\sigma_H/\sigma_{H_2})-1]\,. \tag{6}$$

The known total neutralization cross sections for H^-+H for $E\approx200$ eV also enable us to determine the *absolute* values of $\sigma_e(E)$ and $\sigma_{CT}(E)$. Alternately, the relative cross sections may be normalized to previous measurements of $\sigma_e(E)$ for H^-+H_2 which have been reported by this laboratory.[24] This latter normalization scheme gives identical results owing to the agreement between the measurements of $\sigma_e(E)$ for H^-+H_2 reported by Gealy *et al.*[22] and Huq *et al.*[24] for $E>65$ eV.

There are two nontrivial sources of noise which are encountered in the experiment. Electronic amplification of the rf leakage from the atomic beam source is minimized

with substantial shielding of the source as well as the detectors and by placing the preamplifiers *in vacuo* adjacent to the particle detectors. In addition, a quarter-wave T (for 36 MHz) is inserted into the output cable to further reduce any residual rf-related noise. The other background signal is due to electrons which arise from collisions of the negative ion beam and uv photons (from the atomic beam source) with surfaces in the collision region. The intensities of these extraneous electrons are determined by simply terminating the target and ion beams, respectively.

The full overlap of the target beam with the ion beam is verified by scanning the target beam across the ion beam and observing that this induces a negligible flux change in the ion and electron detectors. Alternatively the same negligible effect can be observed by slightly changing the voltage across the two curved tracks, therefore sweeping the ion beam across the target beam. The target beam density is chosen such that the attenuation of the ion beam is less than 5%; therefore the effects of multiple collisions are negligible.

The measurements determined with the crossed-beam apparatus are repeatable to within 10%. Using the transmission functions determined with H^-+O_2, previous cross-section measurements for electron detachment in H^-+H_2 (Ref. 24) and charge transfer and electron detachment in D^-+O_2 (Ref. 25) can be reproduced with this apparatus to well within their reported experimental uncertainties. The uncertainty in the ratio σ_H/σ_{H_2} at $E=125$ eV, as reported by Gealy *et al.*, is $\pm 10\%$; our determination of the dissociation fraction is reproducible to within $\pm 5\%$. Additional uncertainties in our experiment amount to less than $\pm 10\%$. Therefore the uncertainty associated with the measured cross sections for H^-+H and D^-+H reported here is determined to be $\pm 15\%$.

III. RESULTS AND DISCUSSION

A. Charge transfer of H^- and D^- with H

The measured cross sections for charge transfer are shown in Fig. 3 as functions of E/m, where E and m are the relative collision energy and reduced mass of the projectiles. As usual in resonant charge transfer, cross sections are very large at low collision energy and decrease rapidly as the collision energy increases. The present results overlap and agree well with the earlier measurements by Hummer *et al.*[15] for $E > 100$ eV.

The features of $\sigma_{CT}(E)$ can be understood with a simple semiclassical model in which the nuclei are assumed to move classically and the electrons adjust adiabatically, remaining in eigenstates of the electronic Hamiltonian. The initial state for the collision, with the "extra" electron on the projectile p, may be written:

$$\Psi_p=(1/\sqrt{2})(\phi_g+\phi_u)\ , \tag{7}$$

where g and u refer to the gerade and ungerade states as depicted in Fig. 1. The states ϕ_g and ϕ_u evolve independently during a collision, accumulating different phase factors. The final state after the collision is

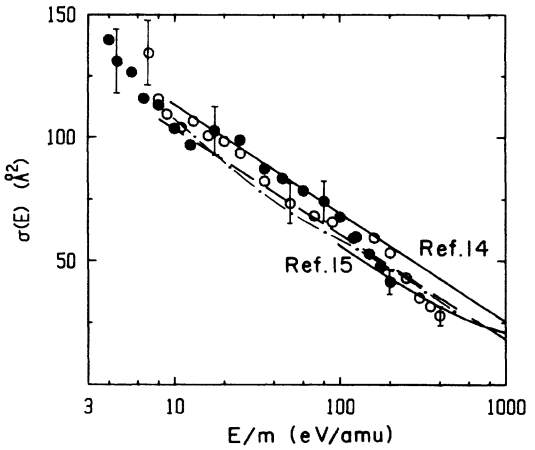

FIG. 3. Total cross sections for charge transfer as a function of E/m for H^-+H (open circles) and D^-+H (closed circles). Also shown are solid lines representative of the experimental results of Ref. 15 and a calculation of Ref. 14; dashed lines, a calculation of Ref. 16; dot-dashed line, the present calculation from Eq. (12) in the text.

$$\Psi_f=(1/\sqrt{2})\left[\phi_g\exp\left[-\frac{i}{\hbar}\int_{-\infty}^{\infty}\varepsilon_g(R)dt\right]+\phi_u\exp\left[-\frac{i}{\hbar}\int_{-\infty}^{\infty}\varepsilon_u(R)dt\right]\right]\ , \tag{8}$$

where $\varepsilon(R)$ is the energy of the particular state as a function of the internuclear separation. Owing to the relative phase, Ψ_f is partially in the charge-transferred state with the extra electron on the target,

$$\Psi_t=(1/\sqrt{2})(\phi_g-\phi_u)\ . \tag{9}$$

The charge-transfer probability for the collision is then $\langle\Psi_t|\Psi_f\rangle^2$, or

$$P=\sin^2\left[\frac{1}{\hbar}\int_0^{\infty}(\varepsilon_g-\varepsilon_u)dt\right]\ . \tag{10}$$

As may be seen in Fig. 1, H_2^- is unstable for small internuclear separations. The lifetime of H_2^- in this unstable region is estimated[10] to be about 10^{-16} s, which is almost one order of magnitude shorter than the collision time. It is thus reasonable to assume unit probability for electron detachment from H_2^- in this region during a collision. Charge transfer is then due to collisions with large impact parameters b. The trajectories of the nuclei for those large impact parameters are approximately straight lines, and by defining $x^2=R^2-b^2$, Eq. (10) can be rewritten as

$$P(b,v)=\sin^2\left[\frac{1}{\hbar v}\int_0^{\infty}(\varepsilon_g-\varepsilon_u)dx\right]\ ; \tag{11}$$

it follows that

$$\sigma_{CT}(E)\approx 2\pi\int_{R_g}^{\infty}P(b,E)b\,db+\frac{\pi}{4}(R_g^2-R_u^2)\ . \tag{12}$$

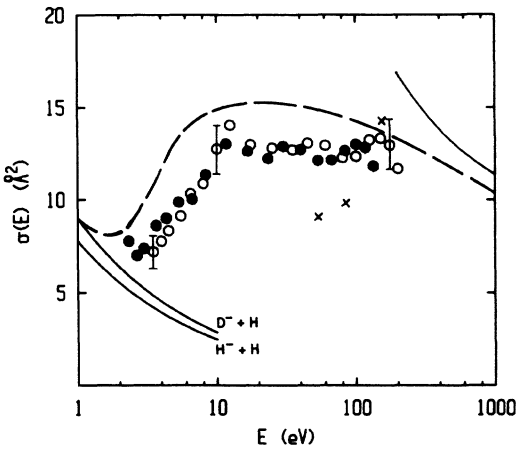

FIG. 4. Total cross sections for electron detachment as a function of the relative collision energy E for H^-+H (open circles) and D^-+H (solid circles). The crosses are the experimental results from Ref. 23 and the solid line summarizes the experimental results of Ref. 15. The dashed line is the calculation of Ref. 6 and the two adjacent solid lines for $E<10$ eV represent the cross sections for associative detachment which have been extrapolated from the low-energy ($E=0.13$ eV) calculation of Ref. 5.

The above equations explain the observed isotope effect of σ_{CT} for the projectiles H^- and D^-.

The potential difference $\varepsilon_g(R)-\varepsilon_u(R)=\Delta(R)$ may be fitted to

$$\Delta(R)=11.4\frac{e^{-0.473R}}{R}, \tag{13}$$

where Δ is in eV and R is in Å and the fitting is done to the calculations of Bardsley *et al.*[9,29] When this expression for $\Delta(R)$ is used in (12) to calculate $\sigma_{CT}(E)$, the result is in excellent agreement with the present measurements, as may be seen in Fig. 3.

The result of an earlier calculation for σ_{CT} (which did not take electron detachment into account) by Dalgarno and McDowell[14] is shown in Fig. 3 as is a subsequent calculation by Bardsley[16] which includes corrections for electron detachment.

B. Electron detachment for H^- and D^-+H

The experimental cross sections for electron detachment $\sigma_e(E)$ are shown in Fig. 4 as functions of relative collision energy. No distinction between direct and associative detachment can be made. The observed behavior of σ_e can be qualitatively understood. As may be seen in Fig. 1, electron detachment may occur as H^- approaches H in the $^2\Sigma_u$ and $^2\Sigma_g$ states which are equally populated. The $^2\Sigma_u$ state crosses into the continuum at $R_u\approx 1.6$ Å and thus becomes unstable for $R<R_u$. The unstable $^2\Sigma_u$ state is a shape resonance, consisting of a $(2p\sigma_u)$ electron bound to a $(1s\sigma_g)^2$ core; it decays into the parent $^1\Sigma_g$ state when the electron tunnels through the p-wave centripetal barrier associated with the $(2p\sigma_u)$ level. The lifetime of the $^2\Sigma_u$ state is about 10^{-16} s based upon the measurements[10] of vibrational excitation of H_2 by low-energy electrons. Thus, the unstable $^2\Sigma_u$ state formed during a collision will decay with almost unit probability, and it contributes to the electron detachment a cross section of $(\pi/2)R_u^2$.

Electron detachment via the $^2\Sigma_g$ state of H_2^- is very similar to that via the $^2\Sigma_u$ state discussed above. The $^2\Sigma_g$ state crosses into the continuum[29] at $R_g\approx 2.6$ Å and for

TABLE I. Charge-transfer and electron-detachment cross sections for collisions of H^- with H and D.

Laboratory collision energy (eV)	Hydrogen target (Å²)		Deuterium target (Å²)	
	σ_e	σ_{CT}	σ_e	σ_{CT}
7	7.2	134	7.8	165
8	7.8	116	7.0	140
9	8.4	110	7.4	131
11	9.1	104	8.6	127
13	10.3	107	9.0	116
16	10.9	101	10.0	113
20	12.8	98	10.0	104
25	14.0	94	11.4	97
35	13.0	82	13.0	103
50	12.8	74	12.6	99
70	12.8	68	12.0	87
90	13.0	66	12.9	84
120	13.0	59	12.7	79
160	12.3	59	12.0	74
200	12.3	53	12.0	68
250	13.0	43	12.7	60
300	13.0	35	13.0	53
350	13.0	32	12.8	48
400	12.7	28	11.8	42

$R < R_g$, it may decay into the parent $^3\Sigma_u$ and $^1\Sigma_g$ states. However, the decay into the $^1\Sigma_g$ state is less probable since the $^2\Sigma_g$ state consists of a $(2p\sigma_u)$ electron bound to a $(1s\sigma_g)(2p\sigma_u)$ core requiring core rearrangement for detachment into the $^1\Sigma_g$ state. This prediction is confirmed by Esaulov[23] in measurements of the energy-loss spectra in $H^- + H$ collisions. The decay $^2\Sigma_g \rightarrow {}^3\Sigma_u$ is very similar to the decay $^2\Sigma_u \rightarrow {}^1\Sigma_g$ and contributes a maximum of $(\pi/2)R_g^2$ to σ_e. Accordingly, if R_g and R_u are taken to be 2.6 and 1.6 Å, an upper limit to the detachment cross section is $\sigma_e \approx 15$ Å^2. This is slightly larger than the present observations for $\sigma_e(E)$ for $E > 10$ eV, suggesting that the crossing radii given above are perhaps too large. A calculation of $\sigma_e(E)$ by Browne and Dalgarno[6] is also shown in Fig. 4; it similarly indicates that the upper limit for σ_e is about 15 Å^2. The decrease in $\sigma_e(E)$ for $E < 10$ eV is due to finite thresholds of the direct detachment channels. Since the $^3\Sigma_u$ state of H_2 is always repulsive, detachment from the $^2\Sigma_g$ state to the $^3\Sigma_u$ state has a threshold in excess of the electron affinity of H.

The cross section for associative detachment $\sigma_{AD}(E)$ has been calculated[5] to be 22 Å^2 for $E = 0.13$ eV. An upper limit for $\sigma_{AD}(E)$ for $E > 0.13$ eV may be estimated by assuming that σ_{AD} is inversely proportional to the collision velocity, i.e., by assuming that the rate constant is independent of the collision velocity. Estimates of $\sigma_{AD}(E)$ which are based upon this assumption are shown in Fig. 4 for $1 < E < 10$ eV. If we subtract this estimated $\sigma_{AD}(E)$ from the observed $\sigma_e(E)$, the resulting cross sections (which are presumably for direct detachment only) are approximately the same for D^- and H^- for a given value of E. This is in accordance with a LCP model for electron detachment in the case where the width of the resonant state is large (i.e., the lifetime is short); this is surely the situation for the H_2^- molecule.

Also shown in Fig. 4 for comparison with the present results are the earlier measurements of σ_e for higher collision energies by Hummer *et al.*[15] and the results of σ_e derived from the differential energy-loss spectra for the $H^- + H$ collisions by Esaulov.[23]

The experimental results for σ_e and σ_{CT} are given in Table I for each of the laboratory collision energies sampled in this experimental investigation. As mentioned earlier, the uncertainty in the cross sections presented in Table I are ±15% for all collision energies.

IV. SUMMARY AND CONCLUSIONS

The cross sections for charge transfer in collisions of H^- and D^- with H display characteristically resonant behavior and a velocity-dependent isotope effect for the H^- and D^- projectiles. The electron-detachment cross sections for the H^- and D^- projectiles are the same when compared at the same collision energies; they are approximately constant from 10 to 200 eV and decrease with decreasing collision energy below 10 eV. The constant cross sections suggest that electron detachment via the H_2^- resonances is saturated for $E > 10$ eV. The decreasing cross sections below 10 eV are probably due to a finite threshold for the detachment from the ionic $^2\Sigma_g$ state to the neutral $^3\Sigma_u$ state.

While the measured cross sections for H^- and $D^- + H$ are reasonably well understood in terms of existing models, a more detailed understanding will require more certainty in the energies of the $^2\Sigma_g$ and $^2\Sigma_u$ states of H_2^-. The difficulty involved in calculating the energies of these states has been discussed in detail by Amaya-Tapia *et al.*[19] They suggest that measurements of differential cross sections for charge transfer would provide a sensitive test for the calculated energy difference between the $^2\Sigma_g$ and $^2\Sigma_u$ states. However, the present results for σ_e imply that the $^2\Sigma_g$ and $^2\Sigma_u$ states do indeed have very short lifetimes which, in turn, implies that the differential cross section for charge transfer will be sharply depleted for large angles. Thus, measurements of these differential cross sections will probably not yield much further information about the potentials for $R < R_g$.

ACKNOWLEDGMENTS

This work was supported in part by the U.S. Department of Energy, Office of Basic Energy Sciences, Division of Chemical Sciences.

[1] C. C. Havener, M. S. Huq, H. F. Krause, P. A. Schulz, and R. A. Paneuf, Phys. Rev. A **39**, 1725 (1989).
[2] B. E. J. Pagel, Annu. Rev. Astron. Astrophys. **2**, 267 (1964).
[3] R. Wildt, Astrophys. J. **89**, 295 (1939).
[4] L. H. Aller and D. B. McLaughlin, *Stars and Stellar Systems* (University of Chicago Press, Chicago, 1965), Vol. VIII, p. 196ff.
[5] R. J. Bieniek and A. Dalgarno, Astrophys. J. **228**, 635 (1979).
[6] J. C. Browne and A. Dalgarno, J. Phys. B **2**, 885 (1969).
[7] A. L. Schmeltekopf, F. C. Fehsenfeld, and E. E. Ferguson, Astron. Phys. Lett. **148**, L155 (1967).
[8] J. N. Bardsley, A. Herzenberg, and F. Mandel, Proc. Phys. Soc. London **89**, 305 (1966).
[9] J. M. Wadehra and J. N. Bardsley, Phys. Rev. Lett. **41**, 1795 (1978); Phys. Rev. A **20**, 1398 (1979).
[10] G. J. Schulz, Rev. Mod. Phys. **45**, 423 (1973).
[11] H. S. W. Massey and R. A. Smith, Proc. R. Soc. London Ser. A **142**, 142 (1933).
[12] N. F. Mott and H. S. W. Massey, *Theory of Atomic Collisions*, 3rd ed. (Oxford University Press, Oxford, 1949).
[13] D. R. Bates, H. S. W. Massey, and A. L. Stewart, Proc. R. Soc. London Ser. A **216**, 437 (1952).
[14] A. Dalgarno and M. R. C. McDowell, Proc. Phys. Soc. London Sec. A **69**, 615 (1956).
[15] D. G. Hummer, R. F. Stebbings, and W. L. Fite, Phys. Rev. **119**, 668 (1960).
[16] J. N. Bardsley, Proc. Phys. Soc. London **91**, 300 (1967).
[17] M. R. C. McDowell and G. Peach, Proc. Phys. Soc. London Sec. A **74**, 463 (1959).
[18] W. Kolos and L. Wolniewicz, J. Chem. Phys. **43**, 2429 (1965).

[19]A. Amaya-Tapia, C. Cisneros, and A. Russek, Phys. Rev. A **34**, 2591 (1986).
[20]See, e.g., J. P. Gauyacq, J. Phys. B **18**, 1859 (1985); C. Mundel, M. Berman, and W. Domcke, Phys. Rev. A **32**, 181 (1985).
[21]J. Geddes, J. Hill, M. B. Shak, T. V. Goffe, and H. B. Gilbody, J. Phys. B **13**, 319 (1980).
[22]M. W. Gealy and B. Van Zyl, Phys. Rev. A **36**, 3091 (1987).
[23]V. A. Esaulov, J. Phys. B **13**, 4039 (1980).
[24]M. S. Huq, L. D. Doverspike, and R. L. Champion, Phys. Rev. A **27**, 2831 (1983).
[25]M. S. Huq, L. D. Doverspike, and R. L. Champion, Phys. Rev. A **27**, 785 (1983).
[26]R. L. Champion and L. D. Doverspike, Phys. Rev. A **13**, 609 (1976).
[27]J. Slevin and W. Sterling, Rev. Sci. Instrum. **52**, 1780 (1981).
[28]Leisk Engineering Limited, Working Instructions of Slevin Atomic Hydrogen Source, Issue 5 (1987), p. 3.
[29]J. N. Bardsley and J. S. Cohen, J. Phys. B **11**, 3645 (1978).